Environmental Science and Pollution Research (2023) 30:55437–55454
https://doi.org/10.1007/s11356-023-26204-0

RESEARCH ARTICLE

Assessment of groundwater quality and human health risks of nitrate and fluoride contamination in a rapidly urbanizing region of India

Riki Sarma[1] · **Santosh Kumar Singh**[1]

Received: 18 August 2022 / Accepted: 25 February 2023 / Published online: 9 March 2023

Abstract
Groundwater contamination studies are important to understand the risks to public health. In this study, groundwater quality, major ion chemistry, sources of contaminants, and related health risks were evaluated for North-West Delhi, India, a region with a rapidly growing urban population. Groundwater samples collected from the study area were analysed for physicochemical parameters — pH, electrical conductivity, total dissolved solids, total hardness, total alkalinity, carbonate, bicarbonate, chloride, nitrate, sulphate, fluoride, phosphate, calcium, magnesium, sodium and potassium. Investigation of hydrochemical facies revealed that bicarbonate was the dominant anion while magnesium was the dominant cation. Multivariate analysis using principal component analysis and Pearson correlation matrix indicated that major ion chemistry in the aquifer under study is primarily due to mineral dissolution, rock-water interactions and anthropogenic factors. Water quality index values showed that only 20% of the samples were acceptable for drinking. Due to high salinity, 54% of the samples were unfit for irrigation purposes. Nitrate and fluoride concentrations ranged from 0.24 to 380.19 mg/l and 0.05 to 7.90 mg/l, respectively due to fertilizer use, wastewater infiltration and geogenic processes. The health risks from high levels of nitrate and fluoride were calculated for males, females, and children. It was found that health risk from nitrate is more than fluoride in the study region. However, the spatial extent of risk from fluoride is more indicating that more people suffer from fluoride pollution in the study area. The total hazard index for children was found to be more than adults. Continuous monitoring of groundwater and application of remedial measures are recommended to improve the water quality and public health in the region.

Keywords Groundwater quality · Hydrogeochemistry · Health risk assessment · Groundwater nitrate · Fluoride contamination · Multivariate analyses

Introduction

Groundwater, as an easily accessible resource, not only meets the domestic water needs of people but also supports agricultural and industrial activities (Jiang et al. 2022). This dependence on groundwater is expected to increase in the future owing to the water demands of a rapidly rising global population (Xiao et al. 2022a). Excessive abstraction of groundwater exceeding the natural recharge inevitably leads to declining groundwater levels, seawater intrusion, land subsidence, and pollution (Wilopo et al. 2021; Orhan 2021). Groundwater pollution is also caused by contaminants released by anthropogenic activities that percolate into subsurface aquifers (Goyal et al. 2021; Motlagh et al. 2020). Assessment of groundwater quality and human health risks related to groundwater pollutants are thus essential research themes for scientists and scholars worldwide (Varol et al. 2021; Snousy et al. 2022).

Major contaminants detected in groundwater are nitrate, fluoride, toxic metals, pesticides, pharmaceuticals, hydrocarbons, and radioactive substances (Bedi et al. 2020; Li et al. 2021a). Researchers around the globe have tested groundwater samples for the presence of such contaminants and evaluated their suitability for drinking and irrigation purposes using geospatial tools, multivariate statistics, and index-based approaches (Sarma and Singh 2021). For example, Rahman et al. (2018) assessed the groundwater quality of Gopalganj district in Bangladesh and reported that most hydrochemical parameters exceeded the limits for

Responsible Editor: Xianliang Yi

Santosh Kumar Singh
sksinghdce@gmail.com

[1] Department of Environmental Engineering, Delhi Technological University, Delhi, India

drinking water standards. For the Guanzhong Basin of northwestern China, Li et al. (2021b) analysed 25 groundwater samples and reported that residents of their study area are at risk from high fluoride levels. Ram et al. (2021) applied water quality index and GIS methods to samples from Uttar Pradesh, India, to categorize the groundwater quality as excellent, good, poor, and unsuitable. For Malda district in Eastern India, water quality assessment showed that 14% of the groundwater samples fell in poor category (Sarkar et al. 2022).

The occurrence of high levels of nitrate and fluoride in groundwater has been reported in many studies (Rezaei et al. 2017; Rufino et al. 2019; Makubalo and Diamond 2020; He et al. 2021; Liu et al. 2022). Nitrate enters the groundwater system from excessive fertilizer use, agricultural runoff, sewage and septic tank leaks, manure systems and animal wastes (Duvva et al. 2022; Dhakate et al. 2023). Consumption of groundwater with nitrate levels greater than 45 mg/L can lead to methemoglobinemia. Also known as blue baby syndrome, this condition reduces the ability of blood to transport oxygen, causing breathlessness, cardiac arrest or death, especially in infants (Ceballos et al. 2021; Golaki et al. 2022; Gugulothu et al. 2022; Panneerselvam et al. 2022). Fluoride naturally occurs in groundwater from geogenic sources and weathering of fluoride-bearing minerals (Subba Rao 2017; Mukherjee and Singh 2018). Surplus application of phosphate fertilizers further enhances the fluoride pollution of groundwater (Karunanidhi et al. 2020; Subba Rao et al. 2021). The intake of fluoride within the permissible limits for drinking water prevents tooth decay and dental cavities and helps in bone formation (Adimalla and Venkatayogi 2017; Sathe et al. 2021). But the long-term intake of excessive fluoride (≥ 1.5 mg/l) may lead to neurological effects, and dental and skeletal fluorosis (Mukherjee and Singh 2018; Ambastha and Haritash 2021; Liu et al. 2022).

In India, high levels of nitrate and fluoride have been reported in many regions — Maharashtra (Nawale et al. 2021), Telangana (Adimalla and Li 2019; Subba Rao et al. 2021; Duvva et al. 2022), Punjab (Singh et al. 2020), Haryana (Kaur et al. 2020; Rishi et al. 2020), Assam (Sathe et al. 2021), Rajasthan (Rahman et al. 2021; Jandu et al. 2021), Tamil Nadu (Karunanidhi et al. 2020; Khan et al. 2021), Jharkhand (Giri et al. 2021) and Uttar Pradesh (Maurya et al. 2020). The United States Environmental Protection Agency has developed a framework to assess the health risks from the usage of fluoride and nitrate contaminated groundwater (USEPA 1989; 1997; 2004; 2014). Many researchers around the world have adopted this model in their studies to evaluate the hazard index (HI) for different categories of people — males, females, children and infants (Singh et al. 2020; Chen et al. 2021; Reddy et al. 2022). The acceptable limit of non-carcinogenic risk is when $HI \leq 1$. If the HI is more than 1, then exposure to contaminated groundwater has serious adverse effects on health (Adimalla et al. 2019). Many studies have reported that infants and children are more at risk than adults (Gao et al. 2020; Adimalla and Qian 2021).

The North-West region of Delhi has industrial, residential and agricultural areas. In the last two decades, this region has experienced major changes in land use. Much of the agricultural lands and rural built-up area have been converted to urban areas. Identifying the mechanisms of groundwater pollution arising from the rapid urbanization in this region is important. This study was carried out in the North-West region of Delhi, India, to (a) evaluate the hydrogeochemistry of groundwater and its suitability for drinking and irrigation, (b) assess the spatial extent of fluoride and nitrate contamination, and (c) estimate the corresponding non-carcinogenic health risks for men, women and children using the USEPA method. The results of this study will be helpful in understanding how increasing urbanization influences groundwater quality and affects human health.

Materials and methods

Study area

The investigated area lies in the North-West region of the National Capital Territory (NCT) of Delhi. The NCT covers a geographical area of 1483 km^2 and falls in the Yamuna River sub-basin, which controls its drainage system. The NCT has adjoining smaller cities — Faridabad, Gurugram, Ghaziabad and Noida which contribute to a total of 3000 km^2 of urban area (Chaudhuri and Sharma 2020). The region is characterized by hot summers and cold winters. The average rainfall is 581 mm. July, August and September are the main monsoon months that receive 81% of the total rainfall. There are planned residential and industrial areas in the North-West region of NCT with some agricultural lands near the adjoining state of Haryana (CGWB n.d). Thus, this area has both urban as well as rural populations. Land use maps from Bhuvan (2021) show that agricultural regions have decreased in the last 15 years while urban areas have increased in this region.

In Delhi, the aquifer geology is complex, varying from Quartzite to Older and Younger Alluvium (CGWB 2021; Sarma and Singh 2022). North West District is characterized by unconsolidated Quaternary alluvium deposits from the Middle to Late Pleistocene Age (CGWB n.d). Sand, silt, and clay are the major soil types in the region in varying proportions. In most of the district, water levels are 5–10 m below ground level, with deeper water levels (> 15 mbgl) observed in the northern part. The district is bordered by the Yamuna River in the northeast which controls the drainage system. The total annual groundwater recharge has been estimated as 8630.7 ham and total annual ground water draft for all uses has been estimated as 9015.2 ham as on 2011 (CGWB n.d). Groundwater exploration studies by the Central Ground Water Board, India, showed that discharge in exploratory wells and piezometers ranged from 150 to 2816 lpm and drawdown ranged from 0.72 to 17.23 m (CGWB n.d). The overall stage of ground water development of the area is 112.36%. The Central Ground Water Board has classified the sub-regions of the district as semi-critical or over-exploited.

Sample collection and analysis

Groundwater samples from 58 locations in the study area were collected from handpumps and bore wells with a depth range of 15–35 mbgl in January 2021. The coordinates of the sampling locations were recorded using a portable GPS device. Location map of the study area and sampling points were prepared by GIS software ArcMap 10.7.1 (Fig. 1). The wells were pumped for 5–10 min to remove the interference from any stagnant water. The water samples were collected in distilled water rinsed polyethylene bottles of 1 l capacity. The sample bottles were sealed, labelled and stored at 4 °C. The analytical procedures for estimating the groundwater parameters were carried out according to the standard methods given by the American Public Health Association (APHA 2017).

The physical parameters — pH, electrical conductivity (EC) and total dissolved solids (TDS) were measured on site using a portable multi-parameter meter (Orion Star A320). Prior to use, the pH meter was calibrated using buffer solutions of pH 4.0, 7.0 and 10.0 and the EC meter was calibrated using standard solutions with EC = 1413 μS/cm and 12.9 mS/cm. Total hardness (TH as $CaCO_3$), total alkalinity (TA as $CaCO_3$), chloride (Cl^-), carbonate (CO_3^{2-}), bicarbonate (HCO_3^-), calcium (Ca^{2+}) and magnesium (Mg^{2+}) ions were determined by titrimetric methods. Sulphate (SO_4^{2-}), nitrate (NO_3^-), and phosphate (PO_4^{3-}) were measured using UV–Visible Spectrophotometers (Labtronics 290 and LabIndia Analytical UV 3092). Fluoride (F^-) was measured using an electrode meter. Sodium (Na^+) and potassium (K^+) ions were determined using a flame photometer (Systronics 128). The analytical test methods, their corresponding reagents and detection limits are presented in Table S1. The accuracy of the chemical analysis was validated by charge balance errors (CBE), and samples with ± 10% error were considered only (Domenico and Schwartz 1990; Adimalla et al. 2019; Rahman et al. 2021; Panneerselvam et al. 2022). Eliminating samples above this error, 52 samples were considered for further analysis (Fig. S1). The CBE was calculated as $\mathrm{CBE} = \frac{\sum \text{cations} - \sum \text{anions}}{\sum \text{cations} + \sum \text{anions}} \times 100$.

The groundwater samples were evaluated for drinking purpose by comparing the observed value against the recommended limits given by the Bureau of Indian Standards (BIS) and World Health Organization (WHO). The spatial distribution maps of the groundwater parameters were created using the inverse-distance weighted (IDW) interpolation technique in ArcMap 10.7.1 software. The

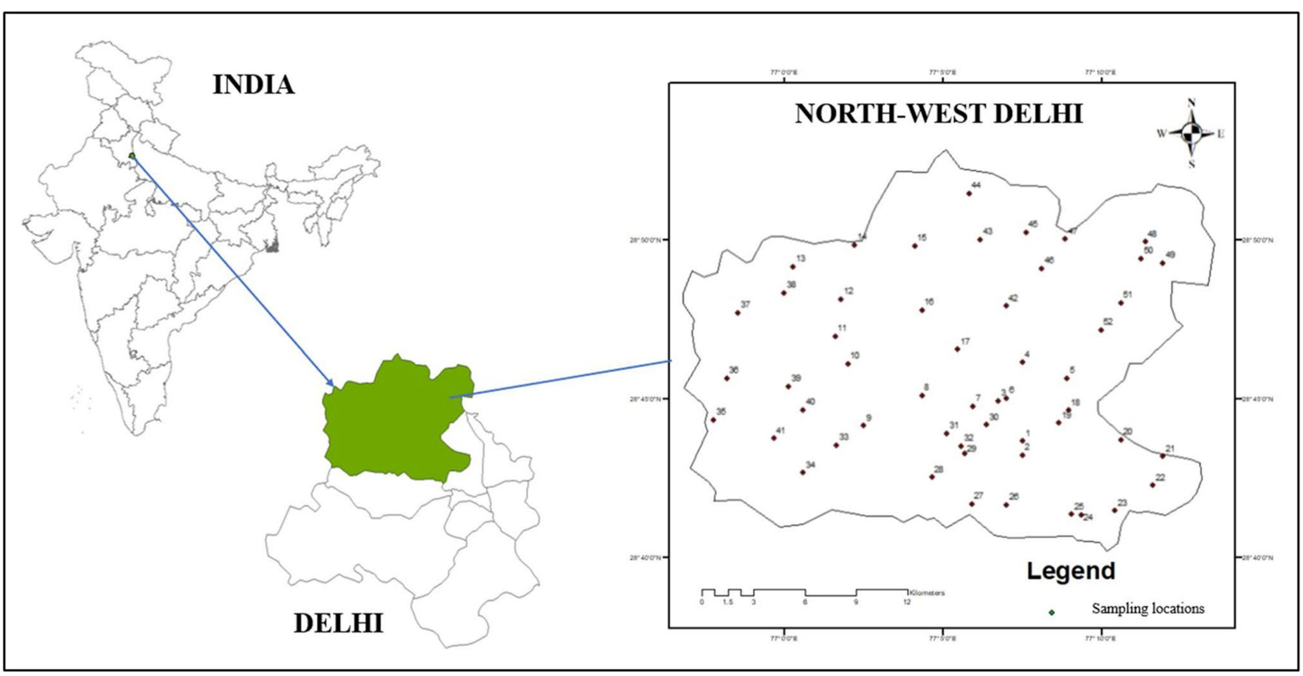

Fig. 1 Groundwater sampling locations in the study area

hydrogeochemical characteristics of the groundwater samples were studied by plotting Piper trilinear diagram (Piper 1944) in AquaChem software. Chloro-alkaline indices CAI-1 and CAI-2 (Schoeller 1965) were calculated to understand the mechanisms of ion-exchange and rock-water interactions (Subba Rao 2017). CAI-1 and CAI-2 were calculated as per the following equations (all ions in meq/l).

$$CAI-1 = \frac{Cl^- - Na^+ + K^+}{Cl^-} \quad (1)$$

$$CAI-2 = \frac{Cl^- - Na^+ + K^+}{SO_4^{2-} + HCO_3^- + CO_3^{2-} + NO_3^-} \quad (2)$$

Water quality index values (WQI) were calculated to determine the suitability of the groundwater samples for drinking. The WQI was based on the values of pH, TDS, TH, TA, Cl^-, F^-, $SO^{2-}{}_4$, $NO^-{}_3$, Ca^{2+}, and Mg^{2+}. The following equation was used to calculate the WQI.

$$WQI = \frac{\sum W_i Q_i}{\sum W_i} \quad (3)$$

where Q_i is the quality rating for each parameter given by $Q_i = 100 * [(V_i - V_o)/(S_i - V_o)]$, V_i is the observed value of ith parameter, V_o is the ideal value of parameter in pure water (0 for all parameters; 7.0 for pH), S_i is the recommended standard value of ith parameter and W_i is the unit weight of each parameter ($W_i = K/S_i$). For calculation of W_i, K is proportionality constant given by $K = 1/\sum(1/S_i)$.

In order to determine the suitability of the samples for irrigation, the parameters such as soluble sodium percentage (SSP), residual sodium carbonate (RSC), sodium absorption ratio (SAR), permeability index (PI), Kelley's ratio (KR) and magnesium hazard (MH) were calculated as per their respective formula (Aravinthasamy et al. 2021) (Table 1). The suitability of samples for irrigation was also determined using the US Salinity Laboratory classification (USSL 1954). IBM SPSS Statistics software version 26 was used for multivariate statistical techniques — principal component analysis (PCA) and Pearson correlation matrix.

Health risk assessment

The USEPA considers high nitrate and fluoride in drinking water as non-carcinogenic risks to human health (USEPA 1989). The exposure routes to such contaminated water may be either through oral ingestion (drinking) and/or dermal contact (bathing). Considering these exposure pathways, the chronic daily intake (CDI in mg/kg/day) through oral ingestion, and dermally absorbed dose (DAD in mg/kg/day) through bathing were calculated. The non-carcinogenic risk through drinking water exposure route in terms of CDI was calculated by Eq. (4).

$$CDI = \frac{CPW * IR * ED * EF}{ABW * AET} \quad (4)$$

where CDI is the chronic daily intake (mg/kg/day), CPW is the concentration of a particular contaminant in groundwater (mg/L), IR is the human ingestion rate (L/day: 2.5 L/day for adults and 0.78 L/day for children), ED is the exposure duration (years: 64, 67 and 12 for men, women and children respectively), EF is the exposure frequency (days/years: 365 days for children and adults), ABW is the average body weight (Kg: 65, 55 and 15 for males, women and children respectively), and AET is the average time (days: 23,360, 24,455 and 4380 for males, women and children, respectively) (USEPA 2014). The health risk due to dermal exposure was calculated by using the following equation.

$$DAD = \frac{CPW * TC * Ki * EV * SSA * CF * ED * EF}{ABW * AET} \quad (5)$$

where DAD is the dermally absorbed dose (mg/kg/day), TC indicates the contact duration (h/d: 0.4 h per day for adults and children), Ki is the dermal adsorption parameters (cm/h: 0.001 cm/h), EV is the bathing frequency (times/day: considered as 1 time in a day), SSA is the skin surface area available for contact (cm^2: 16,600 and 12,000 cm^2 for adults and children, respectively), CF is the unit conversion factors (0.001), ED is the exposure duration (years: 64, 67 and

Table 1 Equations to calculate suitability of water for irrigation

Equations	References
Soluble sodium percentage (SSP) = $[Na^+/(Ca^{2+} + Mg^{2+} + Na^+ + K^+)] * 100$	Wilcox (1955)
Residual sodium carbonate (RSC) = $(HCO_3^- + CO_3^{2-}) - (Ca^{2+} + Mg^{2+})$	Eaton (1950)
Sodium absorption ratio (SAR) = $Na^+/[(Ca^{2+} + Mg^{2+})/2]^{1/2}$	Richards (1954)
Permeability index (PI) = $[Na^+ + (HCO_3^-)^{1/2}/(Ca^{2+} + Mg^{2+} + Na^+)] * 100$	Doneen (1964)
Kelley's ratio (KR) = $Na^+/(Ca^{2+} + Mg^{2+})$	Kelley (1940)
Magnesium hazard (MH) = $[Mg^{2+}/(Ca^{2+} + Mg^{2+})] * 100$	Raghunath (1987)

All ions in meq/l

12 for males, women and children, respectively), EF is the exposure frequency (days/years: 365 days for children and adults), ABW is the average body weight (Kg: 65, 55 and 15 for men, women and children respectively), and AET is the average time (days: 23,360, 24,455 and 4380 for males, women and children, respectively) (USEPA 1997; Adimalla and Qian 2021).

Oral and dermal hazard quotient for the nitrate and fluoride were computed by the following equations:

$$HQ_{oral} = \frac{CDI}{RfD} \quad (6)$$

$$HQ_{dermal} = \frac{DAD}{RfD} \quad (7)$$

where HQ_{oral} and HQ_{dermal} are the non-carcinogenic oral and dermal hazard quotient, respectively. CDI and DAD are chronic daily intake (mg/kg/day) and the dermally absorbed dose (mg/kg/day), respectively, and RfD represents the reference dose of a specific contaminant (USEPA 1989). The oral reference dose of nitrate is 1.6 mg/kg/day and that of fluoride is 0.06 mg/kg/day, obtained from the database of IRIS (Integrated Risk Information System) (USEPA 1989). The HQ values can be used to evaluate the health risk alone where adverse health effects are seen if HQ > 1. However, the hazard index (HI) gives the total hazard presented by exposure to multiple contaminants through multiple pathways. In this study, it is calculated as the sum of the hazard quotients calculated for oral and dermal risk exposure (HQ_{oral} and HQ_{dermal}) to nitrate and fluoride given by:

$$HI_i = HQ_{oral} + HQ_{dermal} \quad (8)$$

$$HI_{total} = \sum_{i=1}^{n} HI_i \quad (9)$$

Based on the HI_{total} values, no significant non-carcinogenic risk occurs if $HI_{total} \leq 1$. However, if $HI_{total} > 1$, then there is significant non-carcinogenic risk (USEPA 1991; 2004).

Results and discussion

Groundwater chemistry

The statistics of the physicochemical parameters of the groundwater samples — minimum, maximum, mean and standard deviation are summarized in Table 2. The pH of the samples ranges between 7.5 and 8.4 with a mean value of 8.0, indicating slightly alkaline conditions. The pH values of the water samples fall within the acceptable limits set by BIS (2012). The EC values vary significantly, with a range of 254–15,440 µS/cm and a mean value of 3699 µS/cm. The

Table 2 Statistics of groundwater quality parameters ($n = 52$) and comparison with drinking water standards (BIS and WHO)

Parameters	Statistics of groundwater samples				Drinking water standards		Percentage of samples exceeding the standard		Maximum multiple of exceeding the standard	
	Minimum	Maximum	Mean	Std. Dev	BIS (2012)	WHO (2017)	BIS	WHO	BIS	WHO
pH	7.5	8.4	8.0	0.22	6.5–8.5	7.0–8.0	–	–	–	–
EC (µS/cm)	254	15,440	3699	3837.68	–	–	-	-	–	–
TDS (mg/l)	128	7770	1854	1922.43	500	600	83%	77%	15.54	12.95
TA as $CaCO_3$ (mg/l)	220	1550	880	312.79	200	–	52%	–	7.75	–
TH as $CaCO_3$ (mg/l)	180	7108	1883	1717.35	200	200	98%	98%	35.54	35.54
Cl^- (mg/l)	20	4700	704	904.81	250	250	58%	58%	18.8	18.8
CO_3^{2-} (mg/l)	0	180	62	41.57	–	–	–	–	–	–
HCO_3^- (mg/l)	268	1696	949	352.80	–	–	–	–	–	–
SO_4^{2-} (mg/l)	35	2840	443	597.78	200	250	58%	50%	14.2	11.36
NO_3^- (mg/l)	0.24	380.19	65.29	89.37	45	50	40%	40%	8.44	7.60
F^- (mg/l)	0.05	7.90	2.23	1.90	1.5	1.5	58%	58%	5.26	5.26
PO_4^{3-} (mg/l)	BDL	0.61	0.13	0.105	–	–	–	–	–	–
Na^+ (mg/l)	4	1006	296	247.47	–	–	–	–	–	–
K^+ (mg/l)	1.4	71.4	12.2	15.09	–	–	–	–	–	–
Ca^{2+} (mg/l)	20	872	170	146.62	75	100	77%	65%	11.62	8.72
Mg^{2+} (mg/l)	20	1580	356	347.15	30	–	96%	–	52.66	–

BDL below detection limit

elevated values of EC indicate high ionic strength, mineral content and dissolved solids. TDS values range from 128 to 7770 mg/l, with a mean value of 1854 mg/l. Only 17% of the samples are within the BIS acceptable limit of 500 mg/l. According to the classification of TDS given by Freeze and Cherry (1979), TDS < 1000 mg/l indicates fresh water while TDS between 1000 to 10,000 mg/l indicates brackish water. Based on this classification, 44% and 56% of the samples fall in the fresh and brackish water categories respectively. Davis and DeWiest (1966) classified groundwater as desirable for drinking if TDS < 500 mg/l, permissible for drinking if TDS is between 500 to 1000 mg/l, useful for irrigation if TDS is between 1000 to 3000 mg/l and unsuitable for drinking and irrigation if TDS > 3000 mg/l. Based on this classification, 17% of the samples were desirable for drinking, 27% were permissible for drinking, 37% were suitable for irrigation and 19% were unfit for both drinking and irrigation. The spatial distribution maps of pH, EC and TDS are given in Fig. S2.

The concentrations of the cations Ca^{2+}, Mg^{2+}, Na^{+} and K^{+} range from 20 to 872 mg/l, 20–1580, 4–1006 and 1.4–71.4 mg/l respectively with mean values of 170, 356, 296 and 12.2 mg/l respectively. The concentrations of dissolved anions such as HCO_3^-, Cl^-, PO_4^{3-} and SO_4^{2-} vary from 268 to 1696, 20 to 4700, 0.00 to 0.61 and 35 to 2840 mg/l respectively with the mean concentrations of 949, 704, 0.13 and 443 mg/l, respectively. The TH values range from 180 to 7108 mg/l as $CaCO_3$ with mean of 1883 mg/l as $CaCO_3$. According to the classification for total hardness by Sawyer and McCarty (1967), water is termed "very hard" if TH > 300 mg/l as $CaCO_3$ and "hard" if TH is between 150 and 300 mg/l as $CaCO_3$. Based on this classification, 92% of the samples have "very hard" water, and 8% of the samples fall in "hard water" categories (Table S2). This is evident from the high levels of bicarbonate ions present in the samples. The standard deviation of SO_4^{2-} is higher than its mean which indicates that sulphate levels in the water samples fluctuate randomly. The dominant major cations in the groundwater samples are in the order of $Mg^{2+} > Na^{+} > Ca^{2+} > K^{+}$, while the dominant anions are $HCO_3^- > Cl^- > SO_4^{2-} > NO_3^- > CO_3^{2-} > F^-$. The elevated concentrations of HCO_3^- along with Mg^{2+} and Ca^{2+} ions in some samples indicate that the study area might be affected by dissolution of carbonate minerals (like calcite and dolomite) and/or silicate minerals by carbonic acid (CGWB 2016; Snousy et al. 2022). Excess Na^{+} over Cl^- indicates rock weathering (or cation exchange) while the vice versa indicates reverse ion exchange (Subba Rao et al. 2017; Gugulothu et al. 2022). For the studied samples, about 85% had excess Cl^- over Na^{+} indicating that reverse ion exchange was the primary source of these ions. High sodium intake (> 200 mg/l) leads to problems of hypertension, kidney and nerves (Rishi et al. 2020). Na^{+}, Mg^{2+} and K^{+} arise from anthropogenic sources such as wastewater, return flows from irrigation and potassium fertilizers (Subba Rao et al. 2021). The high Cl^- concentration may be due to the release of untreated sewage and industrial effluents in the region. Chloride imparts a salty taste to the water and may have laxative effects. The industrial activities in the study region may also be the reason for the high SO_4^{2-} levels found in the water samples. High sulphate concentrations along with high Mg^{2+} are known to cause gastro-intestinal problems (CGWB 2016).

Nitrate levels in the samples range from 0.24 to 380.19 mg/L, with a mean of 65.29 mg/L (Fig. S3(a)). According to WHO (2011), there is no health risk for humans if nitrate levels are below 45 mg/l. However, nitrate between 45 and 100 mg/L causes health effects on children and adults and > 100 mg/L have very high health risk. As per this classification of nitrate, 60% of groundwater samples fall under the "no health risk" category, while 19% and 21% of groundwater samples fall under the "high health risk" and "very high health risk" categories. The spatial distribution map of nitrate is presented in Fig. 2a. Nitrate is predominant in shallow aquifers and easily reaches the groundwater from the surface owing to its high solubility in water (Adimalla and Qian 2021). Nitrate is thus largely anthropogenic in nature and majorly sourced from agrochemicals, open land dumping, domestic, animal and manufacturing wastes (Duvva et al. 2022; Panneerselvam et al. 2022). The high levels of nitrate in the study region may be due to fertilizers such as diammonium phosphate and urea which are commonly utilized in North India. Because of the widespread use of such fertilizers, nitrate can drain away from soils and percolate into the groundwater. Rahman et al. (2021) lists landfill leachate as one of the contributors to nitrate contamination of groundwater. The Bhalaswa landfill in the study region has been operational since 1993 (Sidhu et al. 2015), and its leachate percolating into the groundwater may also contribute to high nitrate levels.

The fluoride concentration ranged from 0.05 to 7.90 mg/l with a mean of 2.23 mg/l (Fig. S3b). Fluoride concentration less than 0.6 mg/l may cause dental caries while greater than 1.5 mg/l may cause severe problems of fluorosis. The concentration of fluoride was below 0.6 mg/l in 21% of the samples and exceeded the permissible limit (1.5 mg/l) in 58% of the groundwater samples. The spatial distribution map of fluoride is presented in Fig. 2b. The high fluoride distribution is identified in northern, southern, central and western parts of the region. Fluoride-rich minerals and usage of phosphate fertilizers are the chief sources of elevated fluoride levels. The anionic exchange controlling the fluoride content in the study region is enhanced by the alkaline nature of water (Duvva et al. 2022; Xiao et al. 2022b). Several studies have reported high concentrations of NO_3^- and F^- in north-west Delhi and the neighbouring state of Haryana

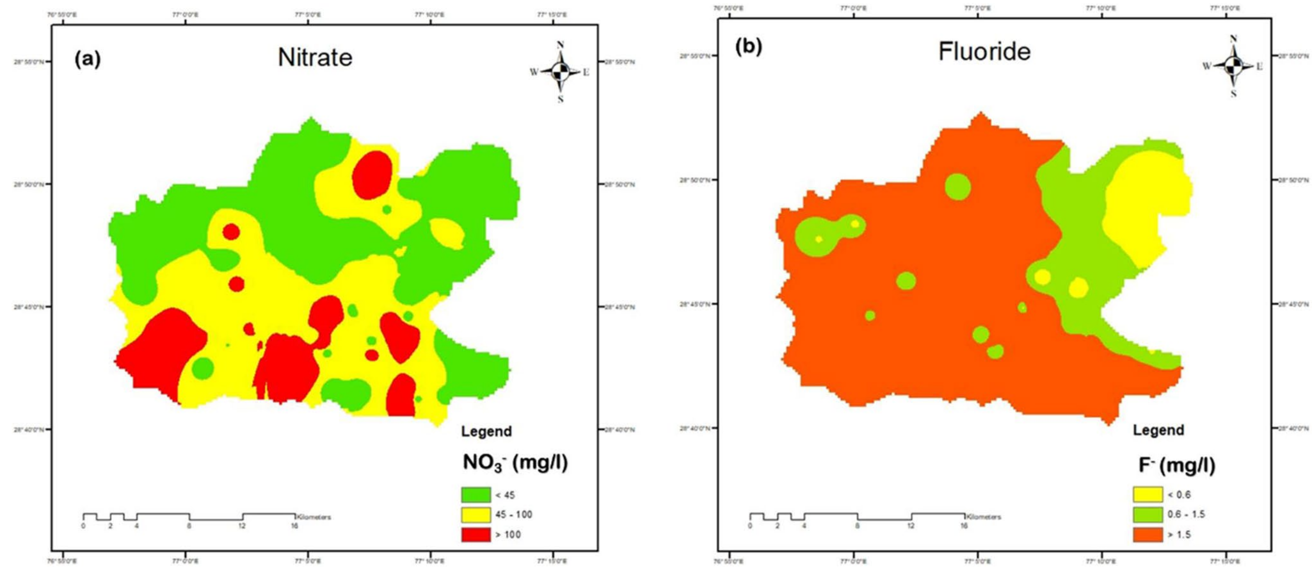

Fig. 2 Spatial distribution maps of **a** nitrate and **b** fluoride in the study area

(Singh et al. 2017; Kaur et al. 2020; Ambastha and Haritash 2021; Masood et al. 2022).

Hydrochemical facies

The Piper trilinear diagram (Piper 1944) suggests the dominance of groundwater chemistry. For the collected groundwater samples, Piper diagram was plotted using AquaChem software, version 10 (Fig. 3). In the cation plot, maximum samples fall in magnesium type (67%) while in the anion plot, maximum samples fall in the bicarbonate type (56%). Mg^{2+} is the dominant ion as a result of weathering of silicate rocks (Adimalla 2019). In the diamond shape, maximum samples (48%) fall in $CaHCO_3$ type followed by mixed CaMgCl type (30%). $CaHCO_3$ type water indicates that River Yamuna and irrigation canals are primarily responsible for the aquifer recharge in the absence of adequate rainfall. The Piper classification indicates that major processes regulating groundwater chemistry in the study region are ion exchanges, rock-water interactions, mineral weathering and anthropogenic influences (Snousy et al. 2022; Panneerselvam et al. 2022).

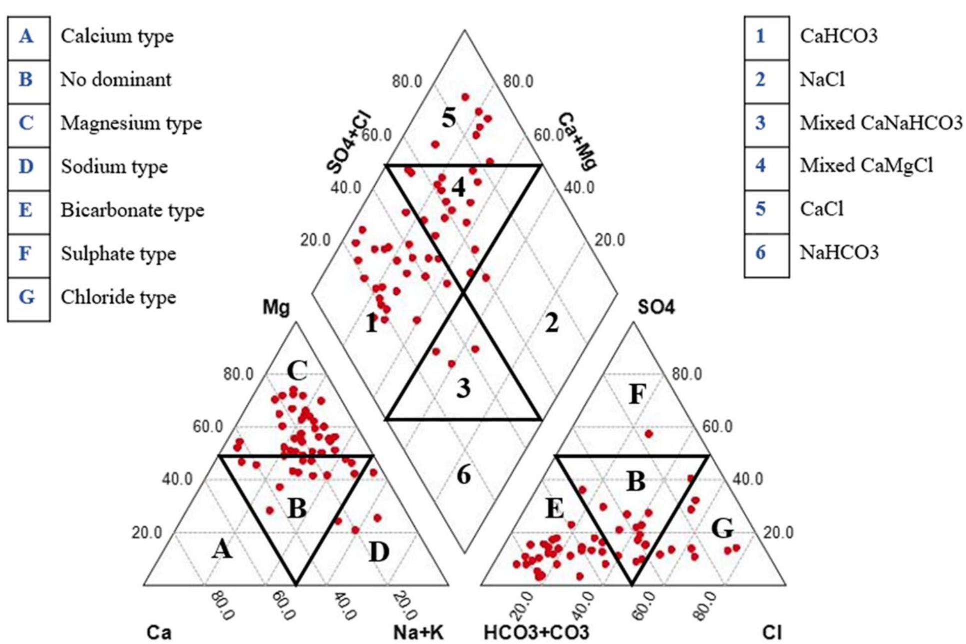

Fig. 3 Piper trilinear classification of groundwater samples

The chloro-alkaline indices CAI-1 and CAI-2 help in understanding the mechanism of ion exchange. If the index is positive, it implies an exchange of sodium and potassium ions from the water with calcium and magnesium ions of the rocks (base–exchange reaction). If it is negative, it indicates vice versa, i.e., calcium and magnesium of water exchanging with sodium and potassium from rocks (cation–anion exchange reaction) (Subba Rao 2017). For the studied groundwater samples, most of the samples demonstrated positive CAI values (Fig. 4a) indicating the cation–anion exchange reaction where Na^+ and K^+ from the water continuously exchanges with Ca^{2+} and Mg^{2+} from aquifer materials due to rock-water interactions (Rashid et al. 2022). Moreover, plot of $(Na^+ + K^+)–Cl^-$ against $(Ca^{2+} + Mg^{2+})–(HCO_3^- + SO_4^{2-})$ can be expressed as $y = -1.1249x + 5.5638$ with a correlation coefficient of 0.9226 (Fig. 4b). The negative slope of − 1.1249 confirms that the relationship between Na^+, K^+, Ca^{2+} and Mg^{2+} is influenced by reverse ion exchange process (Kumar and James 2016):

$$2Na^+ + Ca^{2+}(Mg)–Clay \rightarrow Na^+–Clay + Ca^{2+} + Mg^{2+}$$

Multivariate statistical analysis

Principal component analysis

The application of PCA was first done by checking the Bartlett's test of sphericity and Kaiser–Meyer–Olkin (KMO) sampling adequacy. PCA requires KMO sampling adequacy to be > 0.50 for the dataset (Snousy et al. 2022). The Bartlett test of sphericity was in accordance with p value < 0.0001, and KMO sampling adequacy was 0.671 for the groundwater samples. These values confirm that the dataset is suitable for PCA. The PCA was performed in SPSS software using varimax rotation method with Kaiser normalization. Factors loading values are classified as weak (0.30–0.50), moderate (0.50–0.75), and strong (> 0.75) (Wu et al. 2020). Table 3 reveals that five significant components are calculated (with eigenvalues > 1), which represent 83% of the total variance. The eigenvalues represent how much variance there is in the dataset, and the variance represents the amount of variation in the dataset that can be attributed to each principal component. Component 1 explains 46.6% of the total variance and has positive loading of EC, TDS, TH, Cl^-, Mg^{2+}, Ca^{2+}, Na^+ and SO_4^{2-} implying that EC and TDS are primary governed by the major cations and anions through mineral dissolution, rock-water interaction, ion-exchange and anthropogenic

Table 3 The main five principal components extracted form groundwater samples

	Component				
	1	2	3	4	5
TDS	0.966				
EC	0.966				
TH	0.944				
Mg	0.929				
Cl	0.916				
Na	0.859				
SO4	0.855				0.331
Ca	0.816			− 0.323	
TA		0.975			
HCO3		0.923			
CO3		0.551		0.361	− 0.458
PO4			0.839		
K			0.764		
F				0.817	
pH	− 0.366			0.551	
NO_3					0.878
Eigenvalue	7.459	2.160	1.383	1.197	1.085
% of variance	46.617	13.497	8.642	7.484	6.783

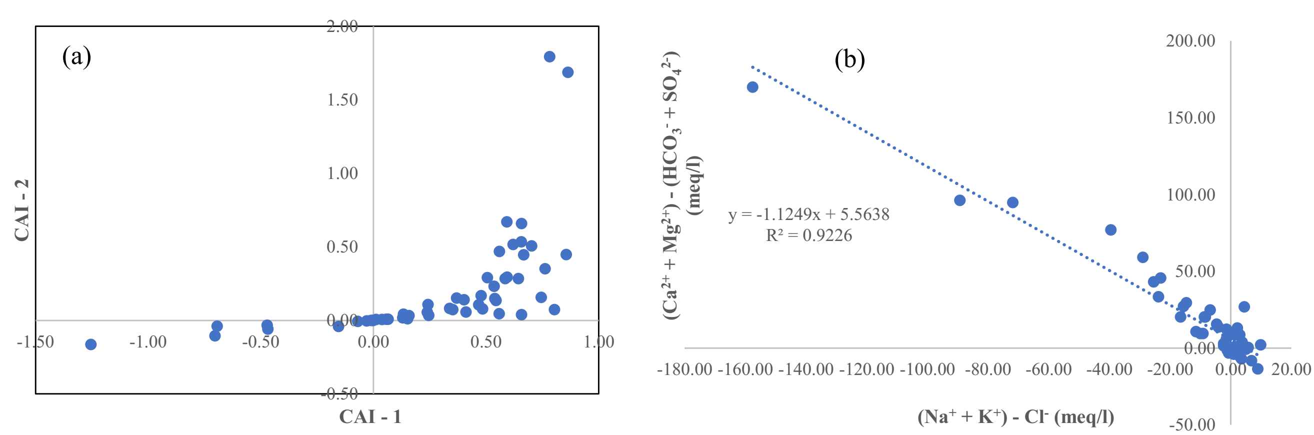

Fig. 4 Plot of **a** CAI-1 against CAI-2 and **b** $(Na^+ + K^+)–Cl^-$ against $(Ca^{2+} + Mg^{2+})–(HCO_3^- + SO_4^{2-})$

factors (Elemile et al. 2021). Component 2 explains 13.5% of the total variance and has positive loading of carbonate, bicarbonate and total alkalinity. This implies that TA is driven by dissolution of carbonate and bicarbonate minerals in the study area. Component 3 explains 8.6% of the total variance and has positive loading of K^+ and PO_4^{3-} indicating the use of potash and phosphate fertilizers. Component 4 explains 7.5% of the total variance and has positive loading of F^-, with moderate loading of CO_3^{2-} and pH and negative loading of Ca. This implies that the concentration of fluoride is due to weathering of fluorite minerals (CaF_2) enhanced by carbonate weathering and alkaline conditions (Barzegar et al. 2017; Xiao et al. 2022b). Finally, component 5 explains 6.8% of the total variance and has strong positive loading of nitrate indicating that origins of nitrate in the water samples may be purely anthropogenic — fertilizer use, sewage and animal wastes. Figure S4 represents the PCA plot of the components in rotated space.

Pearson correlation matrix analysis

The relationships between the physicochemical parameters were analysed by PCMA. The correlation matrix is presented in Table 4. pH has negative correlation with EC, TDS, TH, Cl^-, SO_4^{2-}, Ca^{2+}, Mg^{2+}, and Na^+, consistent with studies by Swain et al. (2022) and Panneerselvam et al. (2021). EC shows identical liner correlation with TDS ($r=1.000$) with a 99% confidence level and significant positive correlation with Na^+ ($r=0.825$), Ca^{2+} ($r=0.835$), Mg^{2+} ($r=0.923$), Cl^- ($r=0.935$) and SO_4^{2-} ($r=0.769$). This is consistent with the results of PCA. The TDS has a strong positive correlation with Na^+ ($r=0.825$) and Cl^- ($r=0.939$) indicating that rock weathering and sewage seepage have caused the salinity to increase. Ca^{2+} shows significant positive correlation with Mg^{2+} ($r=0.756$), Cl^- ($r=0.828$) and SO_4^{2-} ($r=0.693$). Mg^{2+} also shows significant positive correlation with Cl^- ($r=0.867$) and SO_4^{2-} ($r=0.823$). These correlations indicate that major ion chemistry in the groundwater samples is influenced by the dissolution of aquifer materials, rock-water interactions and domestic wastewater infiltration (Snousy et al. 2022). NO_3^- shows negative correlation with pH which is also reported in Stylianoudaki et al. (2022) and Glass and Silverstein (1998).

Water quality index for drinking

Based on the classification given in the study by Masood et al. (2022), the WQI obtained for the groundwater samples were evaluated (Table S3). The WQI < 50 is beneficial for health ("excellent" category) which is calculated for 12% of the samples, located in some isolated pockets in the study region. WQI between 50 and 100 is acceptable for drinking use ("good" category) which is calculated for 8% of the samples. Forty percent of the samples were impure with WQI 100–200 ("poor" category), and 25% of the samples needed treatment prior to use ("very poor" category) with WQI 200–300. The WQI > 300 were found in 15% of the samples which were completely unsuitable for drinking. The spatial distribution map of WQI is presented in Fig. 5. Poor, very poor and unsuitable water quality can be observed in most parts of the study region — central, northern, western, eastern and southern. Only a small area in the north eastern region has good water quality.

Irrigation water quality

Agricultural areas in the study region are situated in the extreme northwest and western regions, where groundwater is the primary source of irrigation. Evaluating the suitability of groundwater for irrigation purposes was done by comparing the irrigation quality parameters with the recommended values (Table 5). The quality of water for irrigation is dependent on its mineral constituents which affect both plants and soil (Wilcox 1955; Alam et al. 2012). The EC is an indicator of the salinity of the groundwater which can influence crop growth. High levels of salinity can negatively affect crop development (Subba Rao 2017; Gugulothu et al. 2022). The salinity is low if EC < 250 μS/cm and very high if EC > 2250 μS/cm. For the study region, 54% of the samples have very high salinity. The sodium absorption ratio (SAR) values indicate the cation–exchange reaction in the soil. High values of SAR specify a situation where the absorbed calcium and magnesium have been replaced by sodium, posing a risk to soil structure (Saha et al. 2019). All the studied samples present a low sodic hazard in terms of the SAR (SAR values < 10). The USSL classification (USSL 1954) plots EC values against the SAR values (Fig. 6). The USSL diagram shows that majority of the samples fall in S1C2, S1C3, S1C4 and S2C4 classes, indicating low to medium sodium hazard and medium to very high salinity hazard in the study region.

The residual sodium carbonate (RSC) is an indicator of the hazardous effects of carbonate and bicarbonate ions for irrigation purposes (Saha et al. 2019; Rishi et al. 2020). RSC values < 1.25 meq/l are fit for irrigation while RSC > 2.5 meq/l are unsuitable. Based on this classification, 83% of the samples are suitable for irrigation while only 15% are unfit. The soluble sodium percentage (SSP) indicates the sodium content in terms of %Na. The sodium-laden water reacts with soil and accumulates in the air spaces (or voids) in the soil. This leads to clogging of the soil particles and reduction in soil permeability which can affect the growth of plants (Todd 1980). The permissible limit of SSP is 60% for irrigation water. Based on this classification, 98% of the samples were permissible for irrigation. Kelley's ratio (KR) measures

Table 4 Pearson correlation coefficient matrix among physicochemical parameters in groundwater samples

	pH	EC	TDS	Cl	CO3	HCO3	SO4	NO3	PO4	F	Ca	Mg	Na	K	TH	TA
pH	1	−0.384**	−0.385**	−0.403**	0.078	−0.215	−0.296*	−0.111	−0.067	0.204	−0.458**	−0.364**	−0.310*	−0.132	−0.400**	−0.182
EC		1	1.000**	0.935**	−0.003	0.203	0.769**	0.169	0.295*	−0.149	0.835**	0.923**	0.825**	0.263	0.943**	0.187
TDS			1	0.939**	−0.001	0.202	0.765**	0.160	0.295*	−0.150	0.834**	0.923**	0.825**	0.264	0.943**	0.186
Cl				1	0.041	0.156	0.619**	0.011	0.274*	−0.185	0.828**	0.867**	0.795**	0.332*	0.896**	0.154
CO3					1	0.235	−0.058	−0.068	0.061	0.182	−0.040	0.026	0.160	−0.008	0.013	0.439**
HCO3						1	0.168	0.285*	0.115	0.053	0.226	0.325*	0.266	0.133	0.318*	0.977**
SO4							1	0.350*	0.022	−0.037	0.693**	0.823**	0.737**	0.118	0.830**	0.142
NO3								1	0.116	0.005	0.154	0.197	0.233	0.240	0.196	0.248
PO4									1	−0.005	0.182	0.172	0.278*	0.399**	0.182	0.120
F										1	−0.243	−0.158	0.036	−0.215	−0.183	0.090
Ca											1	0.756**	0.627**	0.417**	0.840**	0.200
Mg												1	0.750**	0.274*	0.990**	0.306*
Na													1	0.171	0.756**	0.282*
K														1	0.316*	0.121
TH															1	0.296*
TA																1

**Correlation is significant at the 0.01 level (2-tailed)

*Correlation is significant at the 0.05 level (2-tailed)

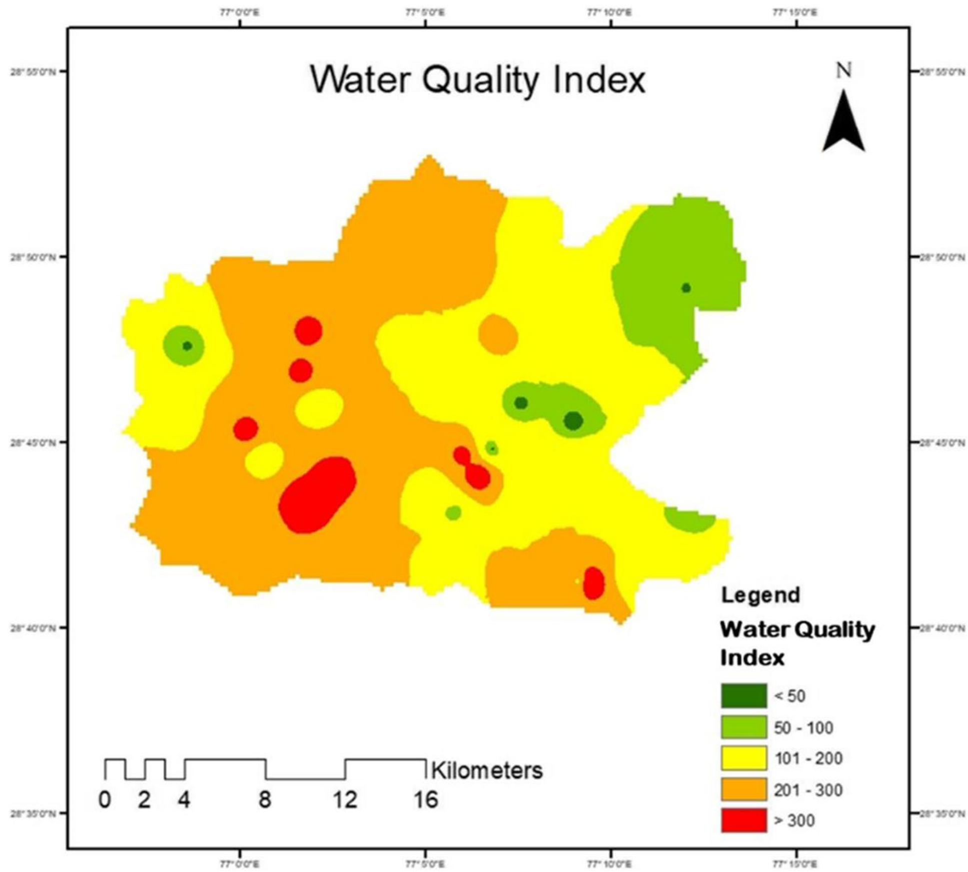

Fig. 5 Spatial distribution map of water quality index

sodium against calcium and magnesium (Kelley 1940). Water with KR > 1 indicates high sodium content and is unsuitable for irrigation. For the present study, KR values ranged from 0.04 to 1.77, with only 4 samples above KR value 1. Ninety-two percent of the samples were within the acceptable limit of KR < 1. Magnesium is important for soil productivity and maintaining soil structure. High levels of magnesium may result due to exchanges with Na^+. This in turn renders the soil alkaline which causes loss of phosphorus (Paliwal 1972; Saha et al. 2019). The magnesium hazard index classifies water for irrigation as suitable if it is < 50 and unsuitable if it is > 50. In the present study, groundwater samples had high levels of Mg^{2+}. Thus 98% of the samples were unsuitable for irrigation (Mg hazard > 50). Permeability of soil is affected by the continuous and long-term use of irrigation water and is regulated by soil Na^+, Mg^{2+}, Ca^{2+} and HCO_3^- (Snousy et al. 2022). The permeability index given by Doneen (1964) classifies water into three classes. Based on this classification, 17% of the samples were unsuitable for irrigation (class III), and 77% and 6% of the samples fall in class II and class I categories, respectively, which are suitable for irrigation.

Health risk assessment for nitrate and fluoride contamination

The groundwater in the study region is used by the local people for irrigation, industrial, and domestic purposes. Many residents in the area use the groundwater for drinking and showering. Since the samples collected had high nitrate and fluoride levels, the estimated concentrations of these pollutants were used for calculating the non-carcinogenic hazard quotient through oral and dermal exposure routes and the total hazard index according to Eqs. (4)–(9). The results obtained for hazard quotients for males, females and children are presented in Table 6.

The risk through dermal contact for nitrate was very low for all 3 categories of people, and the values were less than 1 for all samples. This result was also observed in studies by Zhang et al. (2018) and Gao et al. (2020). The total hazard quotient for nitrate ranged from 0.006 to 9.163 (mean = 1.574) for males, 0.007 to 10.829 (mean = 1.860) for females and 0.010 to 15.917 (mean = 2.734) for children. The $HQ_{nitrate}$ was greater than 1 for 44%, 46% and 52% of the samples for males, females and children respectively. Similar to nitrate, the risk through dermal exposure

Table 5 Irrigation quality of groundwater samples

Parameter	Classification	% of groundwater samples
Electrical conductivity (µS/cm)		
< 250	Low	0
250–750	Medium	13
750–2250	High	33
> 2250	Very high	54
Sodium absorption ratio		
0–10	Low sodic hazard (S1)	100
10–18	Medium sodic hazard (S2)	
18–26	High sodic hazard (S3)	
> 26	Very high sodic hazard (S4)	
Residual sodium carbonate (meq/l)		
< 1.25	Good	83
1.25 – 2.5	Doubtful	2
> 2.5	Unsuitable	15
Soluble sodium percentage (%)		
< 20	Excellent	23
20–40	Good	63
40–60	Permissible	12
60–80	Doubtful	2
> 80	Unsuitable	0
Kelley's ratio		
< 1	Good quality	92
> 1	Unsuitable	8
Magnesium hazard		
< 50	Suitable	2
> 50	Unsuitable	98
Permeability index		
Class I (> 75%)	Suitable	6
Class II (25–75%)	Good	77
Class III (< 25%)	Unsuitable	17

of fluoride was very low, demonstrating that the main health risk is through direct consumption. The total $HQ_{fluoride}$ ranged from 0.031 to 5.078 (mean = 1.433) for males, 0.037 to 6.001 (mean = 1.693) for females and 0.055 to 8.820 (mean = 2.489) for children. $HQ_{fluoride} > 1$ was observed for 58%, 58% and 69% of the samples for males, females, and children respectively. The HQ for nitrate was found to be greater than the $HQ_{fluoride}$ values across all demographics, indicating that nitrate poses a higher health risk to the residents of the study region. However, the percentage of samples with HQ > 1 was more for fluoride indicating that the spatial extent of risk was more for fluoride. The spatial distribution of zones with high health risks is presented in Fig. 7a and b.

The total hazard index (HI_{total}) is a summary of the total risks posed by high levels of nitrate and fluoride (Table 7). For the studied groundwater samples, the HI_{total} was found to be greater than 1 for 75%, 79% and 85% for males, females and children respectively. This indicates that the majority of the population in the study area are at some health risk, primarily from consumption of contaminated groundwater. The spatial distribution map presenting the risk zones are given in Fig. 7c. The values of HI_{total} also indicate that the risk is of the order of children > females > males. Owing to their weak resilience and higher consumption per unit of body weight, children are at a greater risk from drinking contaminated water in the study region than adults (Chen et al. 2016; Adimalla 2020; Guo et al. 2022; Xiao et al. 2022a).

Conclusions

This study analysed the groundwater quality and associated health risks in North-West Delhi, India, which is a rapidly urbanizing region. The hydrogeochemical mechanisms influencing the major ion chemistry were

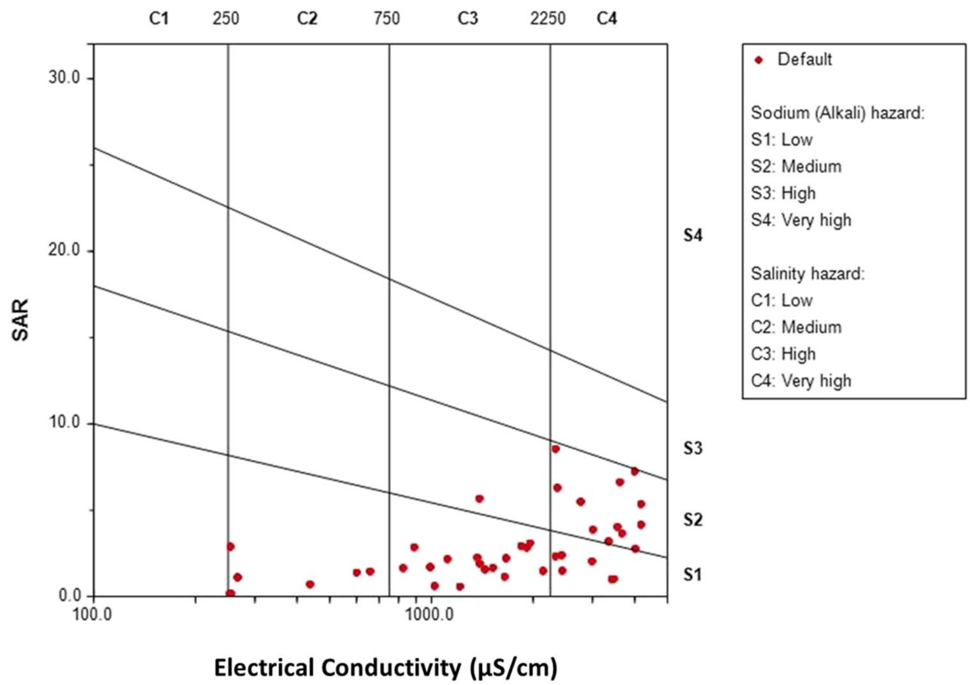

Fig. 6 Groundwater suitability for irrigation according to USSL classification

Table 6 Hazard quotient for (a) nitrate and (b) fluoride

(a)	$HQ_{nitrate\ (oral)}$			$HQ_{nitrate\ (dermal)}$			$HQ_{nitrate\ (total)}$		
	Males	Females	Children	Males	Females	Children	Males	Females	Children
Min	0.006	0.007	0.010	0.000	0.000	0.000	0.006	0.007	0.010
Max	9.139	10.801	15.841	0.024	0.029	0.076	9.163	10.829	15.917
Mean	1.570	1.855	2.720	0.004	0.005	0.013	1.574	1.860	2.734
(b)	$HQ_{fluoride\ (oral)}$			$HQ_{fluoride\ (dermal)}$			$HQ_{fluoride\ (total)}$		
	Males	Females	Children	Males	Females	Children	Males	Females	Children
Min	0.031	0.037	0.054	0.000	0.000	0.000	0.031	0.037	0.055
Max	5.064	5.985	8.778	0.013	0.016	0.042	5.078	6.001	8.820
Mean	1.429	1.689	2.477	0.004	0.004	0.012	1.433	1.693	2.489

explored, and the characteristic pollutants were identified. The dominant cations in the groundwater samples were $Mg^{2+} > Na^{+} > Ca^{2+} > K^{+}$, while the dominant anions were $HCO_3^- > Cl^- > SO_4^{2-} > NO_3^- > CO_3^{2-} > F^-$. The groundwater is slightly alkaline and TDS, TA, TH, Cl^-, SO_4^{2-}, Ca^{2+} and Mg^{2+} exceeded the prescribed drinking water limits in 83%, 100%, 98%, 58%, 58%, 77% and 96% of the analysed samples, respectively. The groundwater in the study region is mostly unsuitable for human consumption.

Piper trilinear diagram showed that maximum samples fell in $CaHCO_3$ type and CaMgCl type categories. The positive value obtained from chloro-alkaline indices showed that Na^+ and K^+ from water exchanged with Ca^{2+} and Mg^{2+} from the aquifer. Multivariate analysis using principal component analysis revealed five significant components which account for 83% of the total variance. Pearson correlation matrix indicated that major ion chemistry is influenced by several factors such as mineral dissolution, rock-water interactions and anthropogenic interferences. The water quality index for drinking was calculated for the collected groundwater samples based on the pH, TDS, TH, TA, Cl^-, F^-, $SO^{2-}{}_4$, $NO^-{}_3$, Ca^{2+}, and Mg^{2+} values, and 15% of the samples were found to be unfit for drinking (WQI > 300). The water samples were analysed for irrigation quality, and results showed that all samples had low sodic hazard. However, 54% of the samples had high salinity, which adversely affects crop production.

Nitrate and fluoride were above the recommended limits of 45 mg/l and 1.5 mg/l in 40% and 58% of the samples, respectively. Wastewater infiltration and fertilizer use are the primary sources of NO_3^- and F^-. High fluoride concentrations in the study region may also be due to geogenic sources. The hazard quotients for nitrate and fluoride suggested that non-carcinogenic health risk is higher

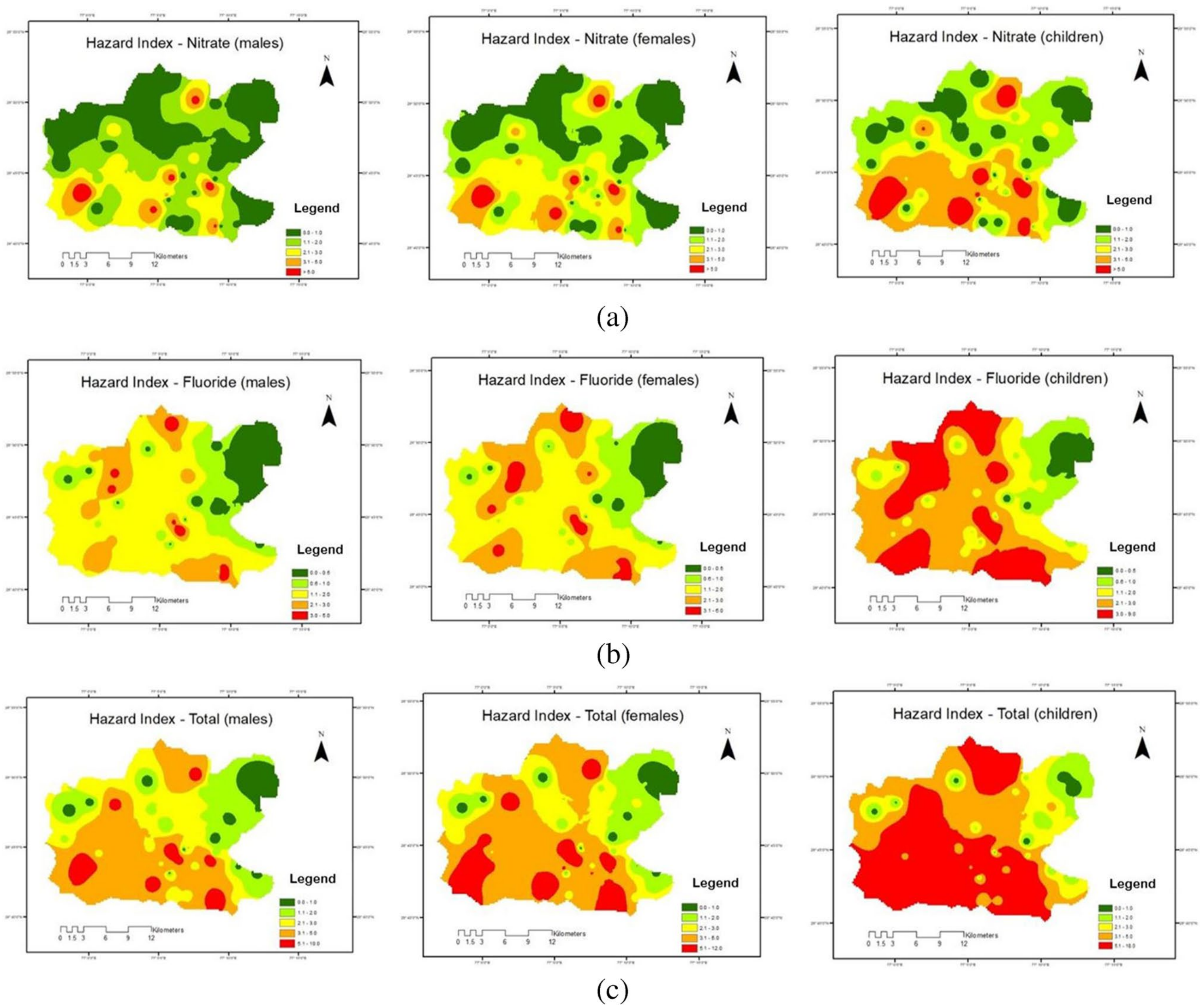

Fig. 7 Spatial distribution of **a** $HI_{nitrate}$, **b** $HI_{fluoride}$, and **c** HI_{total} in the study area

Table 7 Total hazard index for nitrate and fluoride through oral and dermal pathways

	Total hazard index (HI_{total})	Health risk	Number of samples	% of samples
Males	≤ 1	No risk	13	25
	> 1	High risk	39	75
Females	≤ 1	No risk	11	21
	> 1	High risk	41	79
Children	≤ 1	No risk	8	15
	> 1	High risk	44	85

for nitrate contamination. However, the spatial extent of HQ > 1 was more for fluoride, implying that more people are affected by fluoride pollution in the study region. Further, it was observed that the total hazard index was in the order of children > females > males. Due to differences in body weight, children are at a greater health risk than adults. Therefore, groundwater in the study region needs to be continuously monitored and should not be used for direct consumption to avoid adverse health effects. This study is helpful in understanding the chemistry of major contaminants in aquifers of regions that are transitioning from rural to urban areas.

Supplementary Information The online version contains supplementary material available at https://doi.org/10.1007/s11356-023-26204-0.

Acknowledgements The authors acknowledge the support of the Delhi Technological University, New Delhi, for providing the facilities for this study. The authors thank Ms. Nimisha Singla and Mr. Kulvendra Patel, students of DTU, for their assistance during sampling.

Author contribution Both authors contributed to the conceptualization and design of this study. Selection of appropriate methodology, sample collection and analysis were performed by Riki Sarma. Santosh Kumar Singh provided supervision of the work. Riki Sarma prepared and edited the original draft of the manuscript, and Santosh Kumar Singh helped in editing and reviewing. The authors have read and approved the final manuscript.

Data availability All the data used in this study appear in the manuscript.

Declarations

Ethical approval Not applicable.

Consent to participate Not applicable.

Consent for publication The authors hereby grant all rights of publication of the manuscript to the publisher.

Competing interests The authors declare no competing interests.

References

Adimalla N (2019) Groundwater quality for drinking and irrigation purposes and potential health risks assessment: a case study from semi-arid region of south India. Expo Health 11:109–123. https://doi.org/10.1007/s12403-018-0288-8

Adimalla N, Li P (2019) Occurrence, health risks, and geochemical mechanisms of fluoride and nitrate in groundwater of the rock-dominant semi-arid region, Telangana State. India Hum Ecol Risk Assess 25(1–2):81–103. https://doi.org/10.1080/10807039.2018.1480353

Adimalla N, Li P, Qian H (2019) Evaluation of groundwater contamination for fluoride and nitrate in semi-arid region of Nirmal Province, South India: a special emphasis on human health risk assessment (HHRA). Hum Ecol Risk Assess 25(5):1107–1124. https://doi.org/10.1080/10807039.2018.1460579

Adimalla N (2020) Spatial distribution, exposure, and potential health risk assessment from nitrate in drinking water from semi-arid region of South India. Hum Ecol Risk Assess 26(2):310–334. https://doi.org/10.1080/10807039.2018.1508329

Adimalla N, Qian H (2021) Groundwater chemistry, distribution and potential health risk appraisal of nitrate enriched groundwater: a case study from the semi-urban region of South India. Ecotoxicol Environ Saf 207. https://doi.org/10.1016/j.ecoenv.2020.111277

Adimalla N, Venkatayogi S (2017) Mechanism of fluoride enrichment in groundwater of hard rock aquifers in Medak, Telangana State. South India Environ Earth Sci 76:45. https://doi.org/10.1007/s12665-016-6362-2

Alam M, Rais S, Aslam M (2012) Hydrochemical investigation and quality assessment of ground water in rural areas of Delhi. India Environ Earth Sci 66(1):97–110. https://doi.org/10.1007/s12665-011-1210-x

Ambastha SK, Haritash AK (2021) Prevalence and risk analysis of fluoride in groundwater around sandstone mine in Haryana, India. Rend Lincei 32(3):577–584. https://doi.org/10.1007/s12210-021-00997-z

APHA (2017) Standard methods for the examination of water and wastewater, 23rd edn. American Public Health Association, Washington, DC

Aravinthasamy P, Karunanidhi D, Subramani T, Roy PD (2021) Demarcation of groundwater quality domains using GIS for best agricultural practices in the drought-prone Shanmuganadhi River basin of South India. Environ Sci Pollut Res 28(15):18423–18435. https://doi.org/10.1007/s11356-020-08518-5

Barzegar R, AsghariMoghaddam A, Adamowski J et al (2017) Comparison of machine learning models for predicting fluoride contamination in groundwater. Stoch Environ Res Risk Assess 31:2705–2718. https://doi.org/10.1007/s00477-016-1338-z

Bedi S, Samal A, Ray C, Snow D (2020) Comparative evaluation of machine learning models for groundwater quality assessment. Environ Monit Assess 192:776. https://doi.org/10.1007/s10661-020-08695-3

Bhuvan (2021) Indian Geo-Platform of ISRO, National Remote Sensing Centre, Indian Space Research Organisation, Government of India. https://bhuvan.nrsc.gov.in/home/index.php. Accessed 05 Jul 2022

BIS (2012) Indian Standard Drinking Water - Specification (second revision), IS:10500. Bureau of Indian Standards, New Delhi, India

Ceballos E, Dubny S, Othax N, Zabala ME, Peluso F (2021) Assessment of human health risk of chromium and nitrate pollution in groundwater and soil of the Matanza-Riachuelo River Basin. Argentina Expo Health 13(3):323–336. https://doi.org/10.1007/s12403-021-00386-9

CGWB (2016) Aquifer mapping and ground water management plan of NCT Delhi. Central Ground Water Board, State Unit Office, Delhi

CGWB (2021) Groundwater yearbook national capital territory, Delhi (2019–2020). Central Ground Water Board, State Unit Office, Delhi

CGWB (n.d.) Ground water information booklet of North-west district, NCT, Delhi. Central Ground Water Board, State Unit Office, Delhi http://cgwb.gov.in/District_Profile/Delhi_districtprofile.html. Accessed 30 June 2022

Chaudhuri RR, Sharma P (2020) Addressing uncertainty in extreme rainfall intensity for semi-arid urban regions: case study of Delhi, India. Nat Hazards 104:2307–2324. https://doi.org/10.1007/s11069-020-04273-5

Chen J, Wu H, Qian H (2016) Groundwater nitrate contamination and associated health risk for the rural communities in an agricultural area of Ningxia, northwest China. Expo Health 8:349–359. https://doi.org/10.1007/s12403-016-0208-8

Chen F, Yao L, Mei G, Shang Y, Xiong F, Ding Z (2021) Groundwater quality and potential human health risk assessment for drinking and irrigation purposes: a case study in the semiarid region of north China. Water 13(6). https://doi.org/10.3390/w13060783

Davis SN, DeWiest RJM (1966) Hydrogeology. John Wiley & Sons, New York, pp 463

Dhakate R, More S, Duvva LK et al (2023) Groundwater chemistry and health hazard risk valuation of fluoride and nitrate enhanced groundwater from a semi-urban region of South India. Environ Sci Pollut Res. https://doi.org/10.1007/s11356-023-25287-z

Domenico PA, Schwartz FW (1990) Physical and chemical hydrogeology. Wiley, New York

Doneen LD (1964) Water quality for agriculture. University of California, Davis, pp 48

Duvva LK, Panga KK, Dhakate R, Himabindu V (2022) Health risk assessment of nitrate and fluoride toxicity in groundwater contamination in the semi-arid area of Medchal, South India. Appl Water Sci 12(1). https://doi.org/10.1007/s13201-021-01557-4

Eaton FM (1950) Significance of carbonates in irrigation waters. Soil Sci 39:123–133

Elemile OO, Ibitogbe EM, Folorunso OP, Ejiboye PO, Adewumi JR (2021) Principal component analysis of groundwater sources pollution in Omu-Aran Community, Nigeria. Environ Earth Sci 80:690. https://doi.org/10.1007/s12665-021-09975-y

Freeze RA, Cherry JA (1979) Groundwater. Prentice Hall Inc, New Jersey

Gao S, Li C, Jia C, Zhang H, Guan Q, Wu X, Wang J, Lv M (2020) Health risk assessment of groundwater nitrate contamination: a case study of a typical karst hydrogeological unit in East China. Environ Sci Pollut Res 27(9):9274–9287. https://doi.org/10.1007/s11356-019-07075-w

Giri S, Mahato MK, Singh PK, Singh AK (2021) Non-carcinogenic health risk assessment for fluoride and nitrate in the groundwater of the mica belt of Jharkhand, India. Hum Ecol Risk Assess 27(7):1939–1953. https://doi.org/10.1080/10807039.2021.1934814

Glass C, Silverstein J (1998) Denitrification kinetics of high nitrate concentration water: pH effect on inhibition and nitrite accumulation. Water Res 32(3):831–839. https://doi.org/10.1016/S0043-1354(97)00260-1

Golaki M, Azhdarpoor A, Mohamadpour A, Derakhshan Z, Conti GO (2022) Health risk assessment and spatial distribution of nitrate, nitrite, fluoride, and coliform contaminants in drinking water resources of Kazerun, Iran. Environ Res 203. https://doi.org/10.1016/j.envres.2021.111850

Goyal D, Haritash AK, Singh SK (2021) A comprehensive review of groundwater vulnerability assessment using index-based, modelling and coupling methods. J Environ Manage. https://doi.org/10.1016/j.jenvman.2021.113161

Gugulothu S, Subba Rao N, Das R, Duvva LK, Dhakate R (2022) Judging the sources of inferior groundwater quality and health risk problems through intake of groundwater nitrate and fluoride from a rural part of Telangana. Environ Sci Pollut Res, India. https://doi.org/10.1007/s11356-022-18967-9

Guo Y, Li P, He X, Wang L (2022) Groundwater quality in and around a landfill in Northwest China: characteristic pollutant identification, health risk assessment, and controlling factor analysis. Expo Health 14:885–901. https://doi.org/10.1007/s12403-022-00464-6

He X, Li P, Wu J, Wei M, Ren X, Wang D (2021) Poor groundwater quality and high potential health risks in the Datong Basin, northern China: research from published data. Environ Geochem Health 43(2):791–812. https://doi.org/10.1007/s10653-020-00520-7

Jandu A, Malik A, Dhull SB (2021) Fluoride and nitrate in groundwater of rural habitations of semiarid region of northern Rajasthan, India: a hydrogeochemical, multivariate statistical, and human health risk assessment perspective. Environ Geochem Health 43(10):3997–4026. https://doi.org/10.1007/s10653-021-00882-6

Jiang W, Sheng Y, Liu H, Ma Z, Song Y, Liu F, Chen S (2022) Groundwater quality assessment and hydrogeochemical processes in typical watersheds in Zhangjiakou region, northern China. Environ Sci Pollut Res 29(3):3521–3539. https://doi.org/10.1007/s11356-021-15644-1

Karunanidhi D, Aravinthasamy P, Priyadarsi DR, Praveenkumar RM, Prasanth K, Selvapraveen S (2020) Evaluation of non-carcinogenic risks due to fluoride and nitrate contaminations in a groundwater of an urban part (Coimbatore region) of South India. Environ Monit Assess 192:102. https://doi.org/10.1007/s10661-019-8059-y

Kaur L, Rishi MS, Siddiqui AU (2020) Deterministic and probabilistic health risk assessment techniques to evaluate non-carcinogenic human health risk (NHHR) due to fluoride and nitrate in groundwater of Panipat, Haryana, India. Environ Pollut 259. https://doi.org/10.1016/j.envpol.2019.1137

Kelley WP (1940) Permissible composition and concentration of irrigation waters. Proc Am Soc Civil Eng 66:07–613

Khan AF, Srinivasamoorthy K, Prakash R, Gopinath S, Saravanan K, Vinnarasi F, Babu C, Rabina C (2021) Human health risk assessment for fluoride and nitrate contamination in the groundwater: a case study from the east coast of Tamil Nadu and Puducherry, India. Environ Earth Sci 80(21). https://doi.org/10.1007/s12665-021-10001-4

Kumar PJS, James EJ (2016) Identification of hydrogeochemical processes in the Coimbatore district Tamil Nadu, India. Hydrol Sci J 61(4):719–731. https://doi.org/10.1080/02626667.2015.1022551

Li P, Karunanidhi D, Subramani T, Srinivasamoorthy K (2021a) Sources and consequences of groundwater contamination. Arch Environ Contam Toxicol 80:1–10. https://doi.org/10.1007/s00244-020-00805-z

Li Y, Li P, Cui X, He S (2021b) Groundwater quality, health risk, and major influencing factors in the lower Beiluo River watershed of northwest China. Hum Ecol Risk Assess 27(7):1987–2013. https://doi.org/10.1080/10807039.2021.1940834

Liu J, Ma Y, Gao Z, Zhang Y, Sun Z, Sun T, Fan H, Wu B, Li M, Qian L (2022) Fluoride contamination, spatial variation, and health risk assessment of groundwater using GIS: a high-density survey sampling in Weifang City, North China. Environ Sci Pollut Res 29(23):34302–34313. https://doi.org/10.1007/s11356-021-18443-w

Makubalo SS, Diamond RE (2020) Hydrochemical evolution of high uranium, fluoride and nitrate groundwaters of Namakwaland, South Africa. J African Earth Sci 172. https://doi.org/10.1016/j.jafrearsci.2020.104002

Masood A, Aslam M, Pham QB, Khan W, Masood S (2022) Integrating water quality index, GIS and multivariate statistical techniques towards a better understanding of drinking water quality. Environ Sci Pollut Res 29(18):26860–26876. https://doi.org/10.1007/s11356-021-17594-0

Maurya J, Pradhan SN, Seema GAK (2020) Evaluation of ground water quality and health risk assessment due to nitrate and fluoride in the Middle Indo-Gangetic plains of India. Hum Ecol Risk Assess 27(5):1349–1365. https://doi.org/10.1080/10807039.2020.1844559

Motlagh AM, Yang Z, Saba H (2020) Groundwater quality. Water Environ Res 92(10):1649–1658. https://doi.org/10.1002/wer.1412

Mukherjee I, Singh UK (2018) Groundwater fluoride contamination, probable release, and containment mechanisms: a review on Indian context. Environ Geochem Health 40:2259–2301. https://doi.org/10.1007/s10653-018-0096-x

Nawale VP, Malpe DB, Marghade D, Yenkie R (2021) Non-carcinogenic health risk assessment with source identification of nitrate and fluoride polluted groundwater of Wardha sub-basin, central India. Ecotoxicol Environ Saf 208. https://doi.org/10.1016/j.ecoenv.2020.111548

Orhan O (2021) Monitoring of land subsidence due to excessive groundwater extraction using small baseline subset technique in Konya, Turkey. Environ Monit Assess 193(4). https://doi.org/10.1007/s10661-021-08962-x

Paliwal KV (1972) Irrigation with saline water. Indian Agricultural Research Institute (IARI) Monograph No. 2 (New Series), IARI, New Delhi, pp 198

Panneerselvam B, Muniraj K, Duraisamy K, Pande C, Karuppannan S, Thomas M (2022) An integrated approach to explore the suitability of nitrate-contaminated groundwater for drinking purposes in a semiarid region of India. Environ Geochem Health. https://doi.org/10.1007/s10653-022-01237-5

Panneerselvam B, Muniraj K, Pande C, Ravichandran N, Thomas M, Karuppannan S (2021) Geochemical evaluation and human health risk assessment of nitrate-contaminated groundwater in an industrial area of South India. Environ Sci Pollut Res. https://doi.org/10.1007/s11356-021-17281-0

Piper AM (1944) A graphical interpretation of water analysis. EOS Trans Am Geophys Union 25:914–928. https://doi.org/10.1029/TR025i006p00914

Raghunath HM (1987) Groundwater, 2nd edn. Wiley Eastern Ltd., New Delhi

Rahman A, Mondal NC, Tiwari KK (2021) Anthropogenic nitrate in groundwater and its health risks in the view of background concentration in a semi-arid area of Rajasthan, India. Sci Rep 11(1). https://doi.org/10.1038/s41598-021-88600-1

Rahman MM, Islam MA, Bodrud-Doza M, Muhib MI, Zahid A, Shammi M, Tareq SM, Kurasaki M (2018) Spatio-temporal assessment of groundwater quality and human health risk: a case study in Gopalganj. Bangladesh Expo Health 10(3):167–188. https://doi.org/10.1007/s12403-017-0253-y

Ram A, Tiwari SK, Pandey HK, Chaurasia AK, Singh S, Singh YV (2021) Groundwater quality assessment using water quality index (WQI) under GIS framework. Appl Water Sci 11(2). https://doi.org/10.1007/s13201-021-01376-7

Rashid A, Ayub M, Khan S, Ullah Z, Ali L, Gao X, Li C, El-Serehy HA, Kaushik P, Rasool A (2022) Hydrogeochemical assessment of carcinogenic and non-carcinogenic health risks of potentially toxic elements in aquifers of the Hindukush ranges, Pakistan: insights from groundwater pollution indexing, GIS-based, and multivariate statistical approaches. Environ Sci Pollut Res. https://doi.org/10.1007/s11356-022-21172-3

Reddy CKVC, Golla V, Badapalli PK, Reddy NBY (2022) Evaluation of groundwater contamination for fluoride and nitrate in Nellore Urban Province, Southern India: a special emphasis on human health risk assessment (HHRA). Appl Water Sci 12(3). https://doi.org/10.1007/s13201-021-01537-8

Rezaei M, Nikbakht M, Shakeri A (2017) Geochemistry and sources of fluoride and nitrate contamination of groundwater in Lar area, south Iran. Environ Sci Pollut Res 24(18):15471–15487. https://doi.org/10.1007/s11356-017-9108-0

Richards LA (1954) Diagnosis and improvement of saline and alkali soils. Soil Sci 78(2):154

Rishi MS, Kaur L, Sharma S (2020) Groundwater quality appraisal for non-carcinogenic human health risks and irrigation purposes in a part of Yamuna sub-basin, India. Hum Ecol Risk Assess 26(10):2716–2736. https://doi.org/10.1080/10807039.2019.1682514

Rufino F, Busico G, Cuoco E, Darrah TH, Tedesco D (2019) Evaluating the suitability of urban groundwater resources for drinking water and irrigation purposes: an integrated approach in the Agro-Aversano area of Southern Italy. Environ Monit Assess 191(12). https://doi.org/10.1007/s10661-019-7978-y

Saha S, Reza AHMS, Roy MK (2019) Hydrochemical evaluation of groundwater quality of the Tista floodplain, Rangpur. Bangladesh Appl Water Sci 9:198. https://doi.org/10.1007/s13201-019-1085-7

Sarkar M, Pal SC, Islam ARMT (2022) Groundwater quality assessment for safe drinking water and irrigation purposes in Malda district, Eastern India. Environ Earth Sci 81:52. https://doi.org/10.1007/s12665-022-10188-0

Sarma R, Singh SK (2021) Simulating contaminant transport in unsaturated and saturated groundwater zones. Water Environ Res 93(9):1496–1509. https://doi.org/10.1002/wer.1555

Sarma R, Singh SK (2022) A comparative study of data-driven models for groundwater level forecasting. Water Resour Manage 36:2741–2756. https://doi.org/10.1007/s11269-022-03173-6

Sathe SS, Mahanta C, Subbiah S (2021) Hydrogeochemical evaluation of intermittent alluvial aquifers controlling arsenic and fluoride contamination and corresponding health risk assessment. Expo Health 13(4):661–680. https://doi.org/10.1007/s12403-021-00411-x

Sawyer CN, McCarty PL (1967) Chemistry for sanitary engineers, 2nd edn. McGraw-Hill, New York

Schoeller H (1965) Qualitative evaluation of groundwater resources. In Methods and techniques of groundwater investigation and development. UNESCO, pp 54–83

Sidhu BS, Sharma D, Tuteja T, Gupta S, Kumar A (2015) Human health risk assessment of heavy metals from Bhalaswa Landfill, New Delhi, India. In: Raju N, Gossel W, Sudhakar M (eds) Management of natural resources in a changing environment. Springer, Cham. https://doi.org/10.1007/978-3-319-12559-6_16

Singh CK, Kumar A, Shashtri S, Kumar A, Kumar P, Mallick J (2017) Multivariate statistical analysis and geochemical modeling for geochemical assessment of groundwater of Delhi, India. J Geochem Explor 175:59–71. https://doi.org/10.1016/j.gexplo.2017.01.001

Singh G, Rishi MS, Herojeet R, Kaur L, Sharma K (2020) Evaluation of groundwater quality and human health risks from fluoride and nitrate in semi-arid region of northern India. Environ Geochem Health 42(7):1833–1862. https://doi.org/10.1007/s10653-019-00449-6

Snousy MG, Wu J, Su F, Abdelhalim A, Ismail E (2022) Groundwater quality and its regulating geochemical processes in Assiut Province. Egypt Expo Health 14(2):305–323. https://doi.org/10.1007/s12403-021-00445-1

Stylianoudaki C, Trichakis I, Karatzas GP (2022) Modeling groundwater nitrate contamination using artificial neural networks. Water 14:1173. https://doi.org/10.3390/w14071173

Subba Rao N (2017) Controlling factors of fluoride in groundwater in a part of South India. Arab J Geosci 10:524. https://doi.org/10.1007/s12517-017-3291-7

Subba Rao N, Deepali M, Dinakar A, Chandana I, Sunitha B, Ravindra B, Balaji T (2017) Geochemical characteristics and controlling factors of the chemical composition of groundwater in a part of Guntur district, Andhra Pradesh, India. Environ Earth Sci 76:747. https://doi.org/10.1007/s12665-017-7093-8

Subba Rao N, Dinakar A, Kumari BK (2021) Appraisal of vulnerable zones of non-cancer-causing health risks associated with exposure of nitrate and fluoride in groundwater from a rural part of India. Environ Res 202. https://doi.org/10.1016/j.envres.2021.111674

Swain S, Sahoo S, Taloor AK (2022) Groundwater quality assessment using geospatial and statistical approaches over Faridabad and Gurgaon districts of National Capital Region, India. Appl Water Sci 12:75. https://doi.org/10.1007/s13201-022-01604-8

Todd DK (1980) Groundwater hydrology, 2nd edn. John Wiley, New York

US Salinity Laboratory (USSL) (1954) Diagnosis and improvement of saline and alkaline soils. Government Printing Office, Washington

USEPA (1989) Risk assessment guidance for superfund, Volume I: Human Health Evaluation Manual (Part A). United States Environmental Protection Agency, Washington, DC

USEPA (1991) Risk assessment guidance for superfund, Volume I: Human Health Evaluation Manual (Part B, Development of Risk-based Preliminary Remediation Goals). United States Environmental Protection Agency, Washington, DC

USEPA (1997) Exposure factors handbook, Volume 1: General Factors. United States Environmental Protection Agency, Washington, DC

USEPA (2004) Risk assessment guidance for superfund, Volume I: Human Health Evaluation Manual (Part E). United States Environmental Protection Agency, Washington, DC

USEPA (2014) Human health evaluation manual, supplemental guidance: update of standard default exposure factors, OSWER Directive 9200.1–120. United States Environmental Protection Agency, Washington, DC

Varol S, Şener Ş, Şener E (2021) Assessment of groundwater quality and human health risk related to arsenic using index methods and GIS: a case of Şuhut Plain (Afyonkarahisar/Turkey). Environ Res 202. https://doi.org/10.1016/j.envres.2021.111623

WHO (2011) Guideline for drinking water quality, 4th edn. World Health Organization, Geneva

WHO (2017) Guidelines for drinking water quality, 4th edn. Incorporating the First Addendum. World Health Organization, Geneva

Wilcox LV (1955) Classification and use of irrigation waters. US Department of Agriculture, New York

Wilopo W, Putra DPE, Hendrayana H (2021) Impacts of precipitation, land use change and urban wastewater on groundwater level fluctuation in the Yogyakarta-Sleman Groundwater Basin, Indonesia. Environ Monit Assess 193(2). https://doi.org/10.1007/s10661-021-08863-z

Wu J, Li P, Wang D, Ren X, Wei M (2020) Statistical and multivariate statistical techniques to trace the sources and affecting factors of groundwater pollution in a rapidly growing city on the Chinese Loess Plateau. Hum Ecol Risk Assess 26:1603–1621. https://doi.org/10.1080/10807039.2019.1

Xiao Y, Hao Q, Zhang Y, Zhu Y, Yin S, Qin L, Li X (2022a) Investigating sources, driving forces and potential health risks of nitrate and fluoride in groundwater of a typical alluvial fan plain. Sci Total Environ 802. https://doi.org/10.1016/j.scitotenv.2021.149909

Xiao Y, Liu K, Hao Q et al (2022b) Occurrence, controlling factors and health hazards of fluoride-enriched groundwater in the lower flood plain of Yellow River, Northern China. Expo Health 14:345–358. https://doi.org/10.1007/s12403-021-00452-2

Zhang Y, Wu J, Xu B (2018) Human health risk assessment of groundwater nitrogen pollution in Jinghui canal irrigation area of the loess region, northwest China. Environ Earth Sci 77:273. https://doi.org/10.1007/s12665-018-7456-9

Publisher's note Springer Nature remains neutral with regard to jurisdictional claims in published maps and institutional affiliations.